

Cavity QED with cold atoms trapped in a double-well potential

Jiang-Ming Zhang, Wu-Ming Liu, and Duan-Lu Zhou
*Beijing National Laboratory for Condensed Matter Physics,
Institute of Physics, Chinese Academy of Sciences, Beijing 100080, China.*

We investigate the interplay dynamics of a Cavity QED system, where the two-level atoms are trapped in a double-well potential, and the cavity mode, with a frequency largely detuned to the atomic level splitting, is driven by a probe laser. The interaction between the center-of-mass motion of the atoms and the cavity mode is induced by the position dependent atom-field coupling. The dynamics of the system is characterized by two distinct time scales, the inverse of the atomic interwell tunneling rate and the inverse of the cavity loss rate. The system shows drastically different (quasi) steady behaviors in the short-time and long-time intervals.

PACS numbers: 03.75.Be, 03.75.Gg, 03.75.Lm, 32.80.Lg

I. INTRODUCTION

The past decade has witnessed great advances in both the fields of cold atoms and cavity quantum electrodynamics (Cavity-QED), and the overlap between the two fields is ever-growing. A remarkable achievement in this direction is the successful coupling of a Bose-Einstein condensate to a quantized field mode of a high-finesse optical cavity [1, 2]. Besides that, deterministic loading of individual atoms in a micro-cavity is demonstrated [3] and submicron positioning of single atoms in the cavity is achieved [3, 4], which allows control of the atom-field coupling via its position-dependence.

Theoretically, Mekhov, Maschler, and Ritsch proposed to probe the superfluid-insulator transition of cold atoms in optical lattices by the transmission spectra of an optical cavity [5]. The atoms couple to a quantized cavity mode dispersively and hence act as some moving refractive media in the cavity. The cavity transmission spectra directly reflects the quantum or classical distributions of the atoms, which characterize the superfluid or insulator phases respectively. This non-destructive proposal exploits the fact that in the domain of strong coupling, even one atom is enough to shift the cavity resonance significantly. Techniques based on this knowledge have been developed to detect the existence of atoms in a cavity [6], and most recently, been employed to study the correlation, statistics and dynamics of matter-wave fields [7].

From the point of view of atomic optics and quantum information, Ref. [5] also provides us with a model of rich coupled atom-field dynamics [8]. The atoms effectively influence the field dynamics by shifting the resonance of the field mode, while in turn the field intensity determines the dipole potential for the atoms. The former effect is essential for the result of Ref. [5] and is treated in detail. However, the latter effect is neglected. The atomic dynamics is avoided by prescribing a state (phase) for the atoms. Furthermore, the interaction and the coupling to the environment may induce entanglement between the atomic and field subsystems, and cause decoherence of the subsystems, respectively. All these aspects of the system are rarely investigated in Ref. [5].

The purpose of this paper is to investigate the dynamics of the composite atom-field system, with the emphasis on the interplay between the two sides, the correlation and the entanglement between them. We shall consider a “two-site version” of the model presented in Ref. [5]. Atoms are trapped in a double-well potential and interact dispersively with a damped and driven field mode. The two traps are placed asymmetric to the field mode so that the atomic tunneling dynamics is coupled to the field dynamics. Under the two-mode approximation, the freedoms of the atoms are reduced to minimum and can be taken into full account. To gain insight into the dynamics of the system, we assume the system starts from an initial state and evolves towards the steady state. We find that this process involves two distinct time scales, one is the atomic tunneling rate and the other the cavity loss rate, with the latter much faster than the former. These two incommensurate time scales lead to distinct temporal structures of the dynamics. In the short-time interval, where the atomic tunneling can be neglected, it is found that the model we consider is analogous to the Dicke model in the dispersive regime, for which a good understanding exists [9]. Detailed analytical results are obtained and, by the way, the main result of Ref. [5] is recovered. In the long-time interval, however, the atomic tunneling plays an important role. Strong population transfer between different atomic states is observed, and the system displays substantially different behavior than in the short-time interval.

This paper is organized as follows. In Sec. II the basic model is introduced and the Hamiltonian of the atom-field system is derived under the two-mode approximation. Then in Sec. III, based on the master equation, the short-time and long-time behaviors are investigated both analytically and numerically. Finally, our results are summarized in Sec. IV. The connection with the Dicke model is discussed in Appendix A and some useful inequalities are derived in Appendix B.

II. BASIC MODEL AND THE HAMILTONIAN

In this work, we consider the combination of a double-well and an optical cavity, two paradigm models in physics. We assume N two-level bosonic atoms with mass m and transition frequency ω_a are trapped in a double-well potential $V(x)$ and loaded in an optical cavity, where they interact with a cavity field mode with frequency ω_c . The cavity is coherently pumped through the mirror by a weak laser with frequency ω_p and amplitude η . We also assume the atom-field detuning is much larger than the atomic spontaneous emission rate and the Rabi frequency. Under this condition, the atomic upper level can be adiabatically eliminated [10, 11], i.e., the atomic internal dynamics is neglected.

After adiabatic elimination of the atomic upper state, the single-atom-plus-field Hamiltonian in the frame rotating at the frequency of the pumping field is [10]:

$$H_0 = H_{ph} + H_s, \quad (1)$$

where H_{ph} is the rotating frame Hamiltonian for the driven field,

$$H_{ph} = -\Delta a^\dagger a + \eta(a + a^\dagger), \quad (2)$$

with $\Delta = \omega_p - \omega_c$ being the pump-cavity detuning, and

$$H_s = \frac{p^2}{2m} + V(x) + u^2(x)(U_0 a^\dagger a), \quad (3)$$

which is the Hamiltonian for a single atom in the superposition of the classical potential $V(x)$ and the quantum potential $u^2(x)U_0 a^\dagger a$ [10]. Here $u(x)$ is the field mode function with its magnitude at the antinode normalized to unity. The parameter $U_0 = g_0^2/(\omega_c - \omega_a)$, with g_0 being the atom-field coupling at the antinode.

The many-atom-plus-field Hamiltonian, taking into account the direct interaction between the atoms which is characterized by the s -wave scattering length a_s , is:

$$H = H_{ph} + \int d^3x \Psi^\dagger(x) H_a \Psi(x) + \frac{1}{2} \frac{4\pi a_s}{m} \int d^3x \Psi^\dagger(x) \Psi^\dagger(x) \Psi(x) \Psi(x), \quad (4)$$

where $\Psi(x)$ is the atomic field operator and we take $\hbar \equiv 1$ here and henceforth. Under the two-mode approximation for the atomic freedoms, the validity of which has been well established Ref. [12, 13], the atomic field operator $\Psi(x)$ has two contributions:

$$\begin{aligned} \Psi(x) &= b_1 w_1(x) + b_2 w_2(x) \\ &= b_1 w(x - x_1) + b_2 w(x - x_2), \end{aligned} \quad (5)$$

Here we assume a symmetric double well with the two minima at x_1 and x_2 . The two modes $w_1(x)$ and $w_2(x)$ are localized in the left and right traps respectively, and satisfy the orthonormal relation $\int d^3x w_i^*(x) w_j(x) = \delta_{ij}$,

$(i, j) = 1, 2$. The operator b_i^\dagger (b_i) ($i = 1, 2$) creates (annihilates) an atom in the mode $w_i(x)$. Substituting Eq. (5) into Eq. (4), and keeping only terms with dominating contributions, we obtain

$$H = H_{ph} + H_a + H_{int}, \quad (6)$$

where H_a is the Hamiltonian for the atomic subsystem,

$$H_a = -t(b_1^\dagger b_2 + b_2^\dagger b_1) + \frac{u}{2}(n_1(n_1 - 1) + n_2(n_2 - 1)). \quad (7)$$

Here we introduce the atom number operators $n_i = b_i^\dagger b_i$ ($i = 1, 2$) and drop the term associated with the zero-point energy. The atomic tunneling rate t and the on-site interaction energy u are defined as

$$-t = \int d^3x w_1^*(x) \left(-\frac{\nabla^2}{2m} + V(x) \right) w_2(x), \quad (8)$$

$$u = \frac{4\pi a_s}{m} \int d^3x |w_{1,2}(x)|^4. \quad (9)$$

H_{int} describes the interaction between the atoms and the field,

$$\begin{aligned} H_{int} &= \int d^3x \Psi^\dagger(x) u^2(x) \Psi(x) (U_0 a^\dagger a) \\ &\simeq (J_1 n_1 + J_2 n_2) (U_0 a^\dagger a), \end{aligned} \quad (10)$$

where the dimensionless coefficients $J_{1,2}$ are defined as

$$J_{1,2} = \int d^3x u^2(x) |w_{1,2}(x)|^2, \quad (11)$$

which reflect the overlap between the atomic modes and the field mode. Note that $J_{1,2}$ are bounded, $0 \leq J_{1,2} \leq 1$, which follows from the normalization conditions of $u(x)$ and $w_{1,2}(x)$. If the field mode $u(x)$ varies slowly in the range of the spread of the atomic modes, we can take the ‘‘tight confinement approximation’’ [5, 14] $J_i \simeq u^2(x_i)$ ($i = 1, 2$). It is clear from Eq. (10) that the interaction between the atoms and the field is twofold. For the atoms, the depths of the two traps are shifted while for the field the energy per photon is renormalized.

We shall discriminate two different cases: (i) $J_1 = J_2$; (ii) $J_1 \neq J_2$. The former case is trivial, because in this case the dynamics of the atoms and the field is decoupled, the field is indifferent to the distribution of the atoms in the two traps. Thus we concentrate on the case $J_1 \neq J_2$. Without loss of generality, we assume $J_1 = 1$, $J_2 = 0$. This is always reasonable mathematically because we can define two effective parameters, $\Delta' = \Delta - U_0 J_2 N$, $U'_0 = U_0(J_1 - J_2)$, and rewrite the Hamiltonian as

$$\begin{aligned} H &= -t(b_1^\dagger b_2 + b_2^\dagger b_1) + \frac{u}{2}(n_1(n_1 - 1) + n_2(n_2 - 1)) \\ &\quad + U'_0 a^\dagger a n_1 - \Delta' a^\dagger a + \eta(a + a^\dagger), \end{aligned} \quad (12)$$

then effectively we have $J_1 = 1$, $J_2 = 0$. Experimentally, excellent control of the position of a single atom relative to the cavity mode has been demonstrated, so atom-field coupling can be tailored as wanted [3, 4, 15, 16]. In the following, we shall omit the prime for notational simplicity.

III. ANALYTICAL AND NUMERICAL ANALYSIS BASED ON MASTER EQUATION

The Hamiltonian derived above controls the coherent evolution of the atom-field system. However, we still have to take the dissipation into account, which comes from the cavity loss in the model we consider. The overall evolution of the system is governed by the master equation:

$$\dot{\rho} = -i[H, \rho] + \kappa(2a\rho a^\dagger - a^\dagger a\rho - \rho a^\dagger a) \equiv \mathcal{L}\rho. \quad (13)$$

Here ρ is the density matrix of the atom-field system in the rotating frame, and κ is the cavity loss rate. Note that generally the frequency of the cavity mode falls in the optical regime, hence the environment can be treated as at zero temperature. The master equation will be our starting point for the rest of the paper.

As for the dynamics of our system, we stress that there are two distinct time scales [11]. One is the inverse of the atomic tunneling rate t^{-1} , the other being that of the cavity loss rate κ^{-1} . They are the characteristic times of the atomic and field subsystems, respectively. In typical experimental situations, κ is of order 10^6 Hz, while t (and u) is of order 10^3 Hz at most [13]. This means that generally there is a hierarchy $t^{-1} \gg \kappa^{-1}$. The identification of two different time scales leads us to classify the dynamics of the system into *short-* and *long-* time behaviors, which correspond to two disjoint time intervals, (i) $0 < \tau \ll t^{-1}$ and (ii) $\tau \gg t^{-1}$, respectively. In the short-time interval, the atomic tunneling is “frozen”. However, we still expect the system to display some non-trivial behaviors, because this time may be long in unit of κ^{-1} . In the long-time interval, the atomic tunneling may eventually give rise to some important results and should be taken into full account. Specifically we divide the Hamiltonian H into tunneling and non-tunneling terms,

$$H = H_t + H_{non}, \quad (14)$$

with

$$H_t = -t(b_1^\dagger b_2 + b_2^\dagger b_1), \quad (15)$$

$$H_{non} = -\Delta a^\dagger a + \eta(a + a^\dagger) + U_0 a^\dagger a n_1 + \frac{u}{2}(n_1(n_1 - 1) + n_2(n_2 - 1)), \quad (16)$$

and rewrite the master equation as

$$\dot{\rho} = -i[H_{non}, \rho] + \kappa(2a\rho a^\dagger - a^\dagger a\rho - \rho a^\dagger a) - i[H_t, \rho]. \quad (17)$$

The last term will be neglected (kept) in the short- (long-) time intervals, respectively. In the following we shall investigate the behavior of the system in the two time intervals both analytically and numerically.

A. Short-time behavior

Let us assume initially the atoms are in the ground state $|G\rangle$ of the Hamiltonian H_a , while the field is in the

vacuum state $|0\rangle_f$, i.e.,

$$\rho(0) = |G\rangle\langle G| \otimes |0\rangle_{ff}\langle 0|. \quad (18)$$

Then at $\tau = 0$ the pump is turned on and the system evolves according to the master equation (13). In general, solving a master equation analytically exactly is a formidable task, so we will resort to numerical methods as we do. However, in the short-time interval, as mentioned above, we may neglect the tunneling term and approximate the master equation by

$$\dot{\rho} = -i[H_{non}, \rho] + \kappa(2a\rho a^\dagger - a^\dagger a\rho - \rho a^\dagger a) \equiv \mathcal{L}_{non}\rho. \quad (19)$$

As pointed out in Appendix A, H_{non} can be mapped into the Dicke model in the dispersive regime, up to some minor differences. The dynamics of the Dicke model in a driven and damped cavity, in the dispersive regime, has been studied in detail in Ref. [9]. Here we shall follow the techniques there.

Under the transformation to another reference frame,

$$\tilde{\rho} = e^{iA\tau} \rho e^{-iA\tau}, \quad (20)$$

$$A = \frac{u}{2}(n_1(n_1 - 1) + n_2(n_2 - 1)), \quad (21)$$

the master equation (19) takes the form

$$\dot{\tilde{\rho}} = -i[\tilde{H}, \tilde{\rho}] + \kappa(2a\tilde{\rho}a^\dagger - a^\dagger a\tilde{\rho} - \tilde{\rho}a^\dagger a), \quad (22)$$

with the simplified Hamiltonian

$$\tilde{H} = -\Delta a^\dagger a + \eta(a + a^\dagger) + U_0 a^\dagger a n_1. \quad (23)$$

Note that \tilde{H} is diagonal in the atomic space. This leads us to expand the density matrix $\tilde{\rho}$ as

$$\tilde{\rho} = \sum_{m,n=0}^N |m\rangle\langle n| \otimes \tilde{\rho}_{mn}, \quad (24)$$

where $|m\rangle \equiv |m, N - m\rangle$ denotes the atomic state with m atoms in the left trap and $(N - m)$ atoms in the right trap, and $\tilde{\rho}_{mn} = \langle m|\tilde{\rho}|n\rangle$, which is still an operator in the field space. The initial values of the $\tilde{\rho}_{mn}$'s are

$$\tilde{\rho}_{mn}(0) = \langle m|G\rangle\langle G|n\rangle \cdot |0\rangle_{ff}\langle 0|. \quad (25)$$

In terms of $\tilde{\rho}_{mn}$, the atomic and field density operators are respectively,

$$\tilde{\rho}_a = \text{tr}_f(\tilde{\rho}) = \sum_{m,n=0}^N \text{tr}_f(\tilde{\rho}_{mn}) |m\rangle\langle n|, \quad (26)$$

$$\tilde{\rho}_f = \text{tr}_a(\tilde{\rho}) = \sum_{m=0}^N \tilde{\rho}_{mm}. \quad (27)$$

It is straightforward to obtain the time evolution equation of the operators $\tilde{\rho}_{mn}$ from the master equation (22),

$$\begin{aligned} \dot{\tilde{\rho}}_{mn} = & -i[-(\Delta - U_0 p)a^\dagger a + \eta(a + a^\dagger), \tilde{\rho}_{mn}] \\ & + \kappa(2a\tilde{\rho}_{mn}a^\dagger - a^\dagger a\tilde{\rho}_{mn} - \tilde{\rho}_{mn}a^\dagger a) \\ & - iU_0 q(a^\dagger a\tilde{\rho}_{mn} + \tilde{\rho}_{mn}a^\dagger a), \end{aligned} \quad (28)$$

where $p = (m + n)/2$, $q = (m - n)/2$. The general solution of this equation is derived in Ref. [9] by applying the dynamical symmetry method. The result is thorough but complicated, so we will cite it only when we have to.

For the diagonal cases with $m = n$, $q = 0$, Eq. (28) reduces to the master equation describing the dynamics of a single field mode subjected to damping and pumping. Up to a constant coefficient, we make the ansatz that the solution of Eq. (28) in this case takes the form

$$\tilde{\rho}_{mm}(\tau) = |\alpha_m(\tau)\rangle_{ff}\langle\alpha_m(\tau)|, \quad (29)$$

where $|\alpha_m(\tau)\rangle_f$ denotes the field coherent state, and $\alpha_m(0) = 0$. Substituting (29) into Eq. (28), after some operator manipulations, we find that the equation is satisfied if

$$\dot{\alpha}_m(\tau) = -(\kappa - i(\Delta - U_0 m))\alpha_m(\tau) - i\eta. \quad (30)$$

This equation is readily solved by

$$\alpha_m(\tau) = \alpha_m(\infty)(1 - e^{-(\kappa - i(\Delta - U_0 m))\tau}), \quad (31)$$

with

$$\alpha_m(\infty) = \frac{-i\eta}{\kappa - i(\Delta - U_0 m)}. \quad (32)$$

Recalling Eqs. (25) and (27), we have the field density operator

$$\tilde{\rho}_f(\tau) = \sum_{m=0}^N |\langle m|G\rangle|^2 |\alpha_m(\tau)\rangle_{ff}\langle\alpha_m(\tau)|, \quad (33)$$

which is an incoherent superposition of a series of coherent states. Due to the atom-field coupling, both the weights of the coherent states and the coherent states themselves, depend on the initial atomic state. For times $\tau \gg \kappa^{-1}$, $\alpha_m(t)$ saturates to the value $\alpha_m(\infty)$ and the field approaches the quasi-steady state

$$\tilde{\rho}_f(\infty) = \sum_{m=0}^N |\langle m|G\rangle|^2 |\alpha_m(\infty)\rangle_{ff}\langle\alpha_m(\infty)|. \quad (34)$$

The average photon number in the quasi-steady state is

$$\langle a^\dagger a \rangle = \sum_{m=0}^N |\langle m|G\rangle|^2 \frac{\eta^2}{\kappa^2 + (\Delta - U_0 m)^2}. \quad (35)$$

Note that the field approaches its quasi-steady state in a time of order κ^{-1} , which is well within the short-time interval $0 < \tau \ll t^{-1}$. This indicates that the analysis above is self-consistent. We refer to this “steady state” of the field as quasi-steady state so as to differentiate it from the true steady state in the long-time interval.

For off-diagonal cases with $m \neq n$, the last term in Eq. (28) is nonzero. As pointed out in Ref. [9, 17], this non-unitary term will result in the complete disappearance of the operators $\tilde{\rho}_{mn}$, that is, the complete coherence loss of the atomic subsystem. Explicitly,

$$|\rho_a^{mn}| = |\text{tr}_f(\tilde{\rho}_{mn})| \propto \exp(-\tau/\tau_{mn}), \quad (36)$$

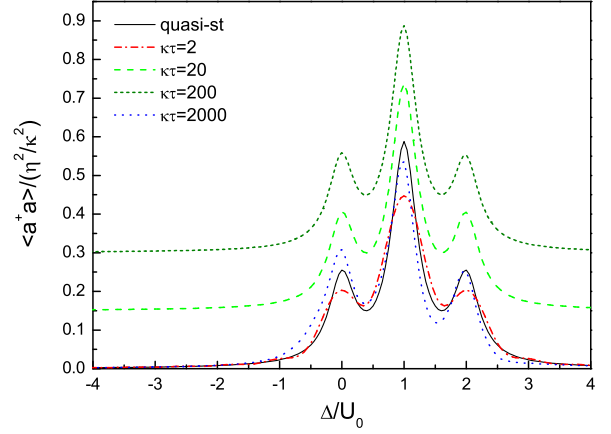


FIG. 1: (color online). Normalized photon number $\langle a^\dagger a \rangle / (\eta^2 / \kappa^2)$ as a function of the pump-cavity detuning Δ , with the master equation cut off at four different times. The quasi-steady state result (solid line) is shown for comparison. The two lines corresponding to $\kappa\tau = (20, 200)$ have been up shifted 0.15 and 0.30 respectively, unless they coincide with the solid line. The parameters are $(t, u) = 2\pi \times (400, 200)\text{Hz}$, $(\kappa, U_0, \eta) = 2\pi \times (1.5, 6.0, 0.1) \times 10^6\text{Hz}$. The number of atoms is $N = 2$.

with the (m, n) -dependent characteristic time

$$\tau_{mn} = \frac{[\kappa^2 + (\Delta - U_0 m)^2][\kappa^2 + (\Delta - U_0 n)^2]}{\kappa U_0^2 \eta^2 (m - n)^2}. \quad (37)$$

If all the τ_{mn} 's are much smaller than t^{-1} , then eventually the atomic subsystem will reach a purely mixed state,

$$\rho_a(\infty) = \sum_{m=0}^N |\langle m|G\rangle|^2 |m\rangle\langle m|, \quad (38)$$

and the atom-field system is merely classically correlated,

$$\rho(\infty) = \sum_{m=0}^N |\langle m|G\rangle|^2 |m\rangle\langle m| \otimes |\alpha_m(\infty)\rangle_{ff}\langle\alpha_m(\infty)|. \quad (39)$$

All the results derived above are based on the approximation that the atomic tunneling is negligible in the short time interval. The quality of this approximation is well demonstrated in Figs. 1 and 2. There we show the time evolution of the photon number and off-diagonal element ρ_a^{01} . The results are obtained by numerically integrating the master equation (13) with the atomic tunneling being taken into account. As shown in Fig. 1, within a time of order κ^{-1} , the photon number builds up and saturates to the value given by Eq. (35). Then it holds on to times of order $10^3/\kappa$ before signatures of deviation from the approximation arise. The excellent agreement between the analytical and numerical results is again demonstrated in the decay of the off-diagonal element ρ_a^{01} in Fig. 2.

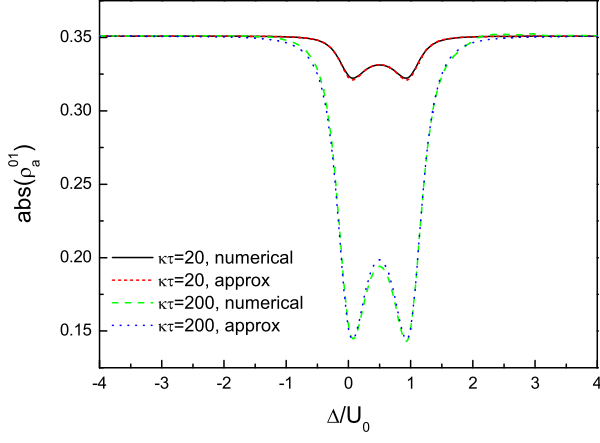


FIG. 2: (color online). Decay of the off-diagonal element ρ_a^{01} at two time sections, $\kappa\tau = (20, 200)$. Analytical approximate results according to Eqs. (36) and (37) and numerical results based on master equation (13) are shown for comparison. The parameters are the same as in Fig. 1.

B. Long-time behavior

As shown above, in the short-time interval, the atomic tunneling can be neglected. However, in the long-time interval, where the system enters the steady state ρ_{st} , the atomic tunneling does play an important role. An analytical exact solution of ρ_{st} is unavailable, so we rely on numerical methods [18]. In Fig. 3 we show the normalized photon number in steady state as a function of the detuning Δ with the pump strength varied. The difference between the long-time steady state result and the short-time quasi-steady state result is apparent. A striking feature of the spectrum in steady state is that the peaks are almost of equal height and in particular, in the weak pump limit ($\eta/\kappa \ll 1$), the height converges to some value around $1/3$ (take into account the overlap between the peaks). In contrast, for the specific set of parameters in our numerical calculations, $(t, u) = 2\pi \times (400, 200)$ Hz and $N = 2$, the quasi-steady state result Eq. (35) predicts the heights of the three peaks to be 0.23, 0.53 and 0.23, respectively. The difference between the steady state and quasi-steady state may be more directly revealed in Fig. 4, where we present the diagonal element ρ_a^{00} and off-diagonal element ρ_a^{01} of the atomic density matrix ρ_a as the detuning and pump strength are varied. From Fig. 4(a) we see that when the detuning is far from all possible resonances, the element ρ_a^{00} is around $1/3$ regardless of the pump strength; and in the limit of weak pump, ρ_a^{00} is around $1/3$ in the whole range of the detuning. From Fig. 4(b) we see the off-diagonal element ρ_a^{01} is far less than unity in the domain of Δ and η we consider. Other diagonal and off-diagonal elements have similar behavior and hence are not shown.

We also investigated the cases with $N \neq 2$, and some common features are found. That is, as long as the condition $(t, u) \ll (\kappa, U_0)$ is fulfilled, in the weak pump

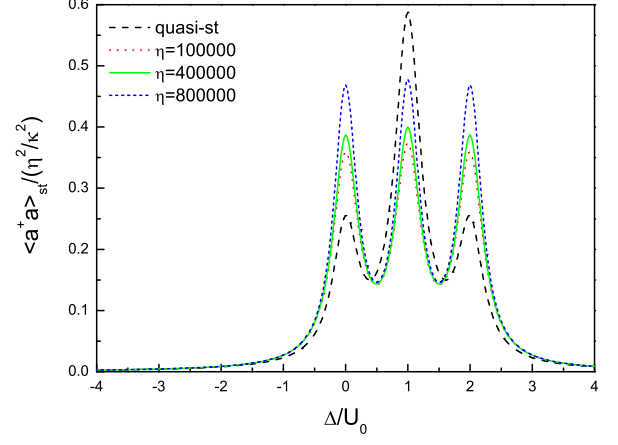


FIG. 3: (color online). Normalized photon number at steady state $\langle a^\dagger a \rangle_{st}/(\eta^2/\kappa^2)$ as a function of the pump-cavity detuning Δ for three different pump strengths. The dashed line corresponding to the quasi-steady state results given by Eq.(35) is shown for comparison. The parameters are the same as in Fig. 1.

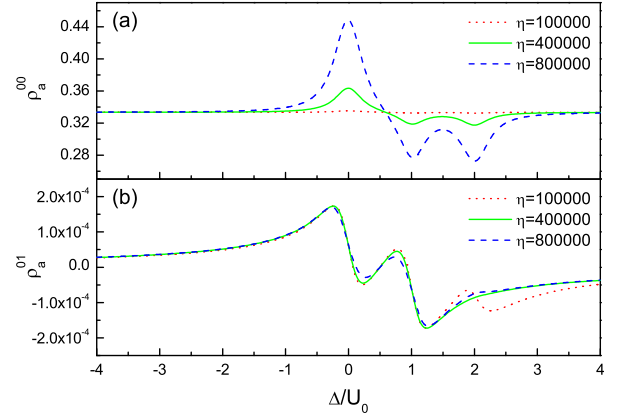


FIG. 4: (color online). (a) Diagonal element ρ_a^{00} and (b) off-diagonal element ρ_a^{01} of the reduced atomic density matrix ρ_a at steady state. The parameters are the same as in Fig. 1.

limit the normalized photon number in steady state $\langle a^\dagger a \rangle_{st}/(\eta^2/\kappa^2)$ as a function of the detuning Δ is the superposition of $N+1$ lorentzians, which are centered at $\Delta = U_0 s$ ($s = 0, 1, \dots, N$), and of heights nearly $1/(N+1)$. Besides that, the diagonal elements of the atomic density matrix converge to values around $1/(N+1)$, while all the off-diagonal elements are vanishingly small, i.e., the atomic subsystem is in a nearly absolutely “unpolarized” mixed state.

The analysis of the short-time behaviors can in fact help us to understand the features of the steady state. The steady state ρ_{st} satisfies

$$0 = \mathcal{L}\rho_{st} = \mathcal{L}_{non}\rho_{st} - i[H_t, \rho_{st}]. \quad (40)$$

Because $t \ll (\kappa, U_0)$, we shall treat the second term as a perturbation over the first term, for which we have analytical results. Assume that

$$\rho_{st} = \rho_{st}^0 + \rho_{st}^1, \quad (41)$$

where ρ_{st}^0 is of zeroth order in t/κ , while components of higher orders in t/κ are included in ρ_{st}^1 . ρ_{st}^0 satisfies the equation $\mathcal{L}_{non}\rho_{st}^0 = 0$. According to the analysis in the previous subsection, its general solution is

$$\rho_{st}^0 = \sum_{m=0}^N C_m |m\rangle\langle m| \otimes |\alpha_m(\infty)\rangle\langle\alpha_m(\infty)|, \quad (42)$$

with the coefficients C_m being arbitrary. Note that ρ_{st}^0 is diagonal in the atomic space, which implies that the off-diagonal elements of the atomic density matrix must come from ρ_{st}^1 and hence are at least of order t/κ . This explains why the off-diagonal elements are vanishingly small as revealed by the numerical calculations. The physical picture is that, via the atom-field coupling and the dissipation, the coherence of the atomic subsystem is greatly depleted, the remaining weak coherence is just due to the finite atomic tunneling.

The knowledge of the off-diagonal elements of the atomic density matrix allows us to understand the behavior of the diagonal elements and the photon number, at least in the weak pump limit. In steady state, we have the following equation for an arbitrary operator \hat{O} ,

$$0 = \langle \dot{\hat{O}} \rangle_{st} = -i\langle [\hat{O}, H] \rangle_{st} + \kappa \langle [a^\dagger, \hat{O}] a - a^\dagger [a, \hat{O}] \rangle_{st}. \quad (43)$$

Let $\hat{O} = |m\rangle\langle m+1|$, $0 \leq m \leq N-1$, then we obtain

$$\begin{aligned} 0 = & f(m+1)(\langle |m\rangle\langle m| \rangle_{st} - \langle |m+1\rangle\langle m+1| \rangle_{st}) \\ & + f(m+2)\langle |m\rangle\langle m+2| \rangle_{st} - f(m)\langle |m-1\rangle\langle m+1| \rangle_{st} \\ & - \frac{u}{t}(2m+1-N)\langle |m\rangle\langle m+1| \rangle_{st} \\ & - \frac{U_0}{t}\langle |m\rangle\langle m+1| a^\dagger a \rangle_{st}, \end{aligned} \quad (44)$$

where $f(m) = \sqrt{(m+1)(N-m)}$. In the weak pump limit, the second and third terms on the right hand side is of order t/κ , the fourth term u/κ , while the fifth term $(\eta/\kappa)^2$, so to zeroth order in t/κ , u/κ and η/κ , we have

$$\langle |m\rangle\langle m| \rangle_{st} - \langle |m+1\rangle\langle m+1| \rangle_{st} = 0. \quad (45)$$

This equation, together with the normalization condition $\text{tr}(\rho_a) = 1$, means that to zeroth order in t/κ , u/κ and η/κ ,

$$\langle |m\rangle\langle m| \rangle_{st} = \frac{1}{N+1}. \quad (46)$$

Returning to Eqs. (41) and (42), we see that in the weak pump limit (the condition $t, u \ll \kappa$ is spontaneously satisfied), the steady state is well approximated by

$$\rho_{st} \simeq \frac{1}{N+1} \sum_{m=0}^N |m\rangle\langle m| \otimes |\alpha_m(\infty)\rangle\langle\alpha_m(\infty)|. \quad (47)$$

The photon number $\langle a^\dagger a \rangle_{st}$ in this limit is given by

$$\langle a^\dagger a \rangle_{st} = \frac{1}{N+1} \sum_{m=0}^N \frac{\eta^2}{\kappa^2 + (\Delta - U_0 m)^2}. \quad (48)$$

Eqs. (46) and (48) account for the weak pump steady state features. In fact the photon number is always directly determined the diagonal elements $\langle |m\rangle\langle m| \rangle_{st}$, not limited to the weak pump limit. Let $\hat{O} = a^\dagger a$ and $a|m\rangle\langle m|$ in Eq. (43), we have

$$\begin{aligned} 0 = & i\eta(\langle a \rangle_{st} - \langle a^\dagger \rangle_{st}) - 2\kappa\langle a^\dagger a \rangle_{st} \\ = & i\eta \sum_{m=0}^N (\langle a|m\rangle\langle m| \rangle_{st} - c.c.) - 2\kappa\langle a^\dagger a \rangle_{st}, \quad (49) \\ 0 = & it\langle [a|m\rangle\langle m|, b_1^\dagger b_2 + b_2^\dagger b_1] \rangle_{st} - i\eta\langle |m\rangle\langle m| \rangle_{st} \\ & - (\kappa - i(\Delta - U_0 m))\langle a|m\rangle\langle m| \rangle_{st}, \end{aligned} \quad (50)$$

where *c.c.* stands for complex conjugate. As shown in Appendix B, the first term on the right hand side of Eq. (50) can be safely neglected compared to the second term. By neglecting it we get a set of algebraic equations of $\langle a^\dagger a \rangle_{st}$, $\langle a|m\rangle\langle m| \rangle_{st}$. We solve

$$\langle a^\dagger a \rangle_{st} \simeq \sum_{m=0}^N \langle |m\rangle\langle m| \rangle_{st} \cdot \frac{\eta^2}{\kappa^2 + (\Delta - U_0 m)^2}, \quad (51)$$

which is valid for arbitrary values of η .

An important question of concern is what is the time scale for the system to approach the steady state. The general solution of a master equation like Eq.(13) with a time-independent Liouvillian can be written as a sum of a series of complex exponentials,

$$\rho(\tau) = \sum_j a_j \exp(s_j \tau), \quad (52)$$

where $s_j = -R_j + iI_j$, ($R_j, I_j \in \mathcal{R}$) are the eigenvalues of the Liouvillian, while the coefficients a_j are determined by the initial conditions. As well known, the Liouvillian is singular and has at least one zero eigenvalue which correspond(s) to the steady state(s), and all the non-zero eigenvalues have negative real parts. This ensures that $\rho(\tau)$ converges to the steady state(s) in the limit of $\tau \rightarrow \infty$. Obviously, the time scale of this process is set by the inverse of the least modulus real part of the eigenvalues. We define

$$\tau_{max} = \max_j \left\{ \frac{1}{R_j}; R_j \neq 0 \right\}. \quad (53)$$

In Fig.5, we show $\kappa\tau_{max}$ as a function of the detuning. Note that $\kappa\tau_{max}$ is of order $10^4 \sim 10^6$ in the regime $|\Delta/U_0| \leq 5$ and it diverges as $|\Delta| \rightarrow \infty$. Compared with Fig. 1, this clearly demonstrates that the long-time and short-time behaviors lie in two well separated time intervals. Moreover, it clarifies a point that, when the pump is far from all possible resonances, the influence of the pump on the system is negligible, so it would take the system a time experimentally unaccessible to reach the steady state. Of course, the situation is still good in the regime $0 \leq \Delta/U_0 \leq 2$, where the time scale is of order 10ms. At present, individual atoms have been trapped and detected in an optical cavity for time scales exceeding 15s [3], so we expect that the steady state features may also have the possibility to be observed in the future.

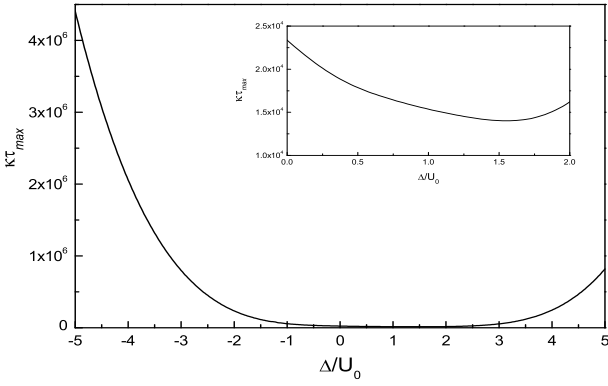


FIG. 5: (color online). Timescale τ_{max} in unit of $1/\kappa$ for the system approaching the steady state. Inset: close-up of the curve in the regime $0 \leq \Delta/U_0 \leq 2$. The parameters are the same as in Fig. 1.

IV. SUMMARY AND REMARKS

We investigated the dynamics of a dispersively interacting atom-field system, with the slowly varying atomic interwell tunneling coupled with the fast varying field dynamics. Depending on the role of the atomic tunneling, the dynamics of the system was classified into short-time and long-time behaviors.

In the short-time interval ($0 < \tau \ll t^{-1}$), as verified by the numerical calculations, the atomic tunneling can be neglected. We recovered the result of Ref. [5] in the “two-site” case, and went beyond to obtain a more detailed picture of the dynamics of the atom-field system, such as the decoherence of the atomic subsystem, the correlation between the atomic and field subsystems. In our analysis, a central observation is the analogy between the model we consider and the well known Dicke model in the dispersive regime. In fact, many results are directly borrowed from previous works on Dicke model [9]. Of course, we stress that this similarity is not essential. It is the dispersive nature of the atom-field coupling that counts. As can be seen from our procedures, similar techniques and results apply also to the many-site cases, e.g., the original model in Ref. [5].

As for the long-time behavior, we were primarily interested in the steady state. If the atomic tunneling is absent, the steady state of the system is in the form of Eq. (42). The atomic and field subsystems are only classically correlated, and the populations of different atomic states are absolutely determined by the initial state. However, the presence of atomic tunneling leads to strong population transfers between the atomic states. A remarkable feature is that, in the weak pump limit, the atomic states are almost equally populated, which is substantially different from the ground state atomic distribution. We also quantitatively investigated the time scale of reaching the steady state and found that it lies well in the long time interval and is accessible under the experimental situations at present.

Finally, we have some remarks about the experimental implementation of the model we discussed in this work. The double-well may be constructed by two adjacent optical dipole traps between which the distance can be adjusted as in Ref. [19]. An important feature of these traps is the extremely small focal spot, a beam waist radius of $w_0 < 1\mu\text{m}$ is achieved. This helps to confine the atom in a very small volume and validate the “tight confinement approximation”. The case $J_1 = 1$, $J_2 = 0$ occurs when one atomic mode is localized in an antinode of the field mode, and the other in a node.

Acknowledgments

We are grateful to P. Zhang and M. Xiao for stimulating discussions and we would also like to thank A. S. Parkins for his help on the programming. This work was supported by NSF of China under grant 90406017, 60525417, 10775176, the NKBRF of China under Grant 2005CB724508, 2006CB921400, 2006CB921206, and 2006AA06Z104..

APPENDIX A: CONNECTION WITH THE DICKE MODEL

In terms of Schwinger’s representation of the angular momentum operators [20],

$$S_x = \frac{1}{2}(b_2^\dagger b_1 + b_1^\dagger b_2), \quad (\text{A1})$$

$$S_y = \frac{i}{2}(b_2^\dagger b_1 - b_1^\dagger b_2), \quad (\text{A2})$$

$$S_z = \frac{1}{2}(b_1^\dagger b_1 - b_2^\dagger b_2), \quad (\text{A3})$$

the Hamiltonian H can be rewritten as

$$H = H_t + H_{non}, \quad (\text{A4})$$

with

$$H_t = -2tS_x, \quad (\text{A5})$$

$$H_{non} = \left(\frac{U_0 N}{2} - \Delta\right)a^\dagger a + \frac{U_0}{2}(2a^\dagger a + 1)S_z + \eta(a + a^\dagger) + u\left(S_z^2 + \frac{N^2}{4} - \frac{N}{2}\right) - \frac{U_0}{2}S_z. \quad (\text{A6})$$

Up to terms diagonal in the S_z -representation, H_{non} corresponds to the Dicke model in the dispersive regime [9], with cavity-pump detuning $(\frac{U_0 N}{2} - \Delta)$, effective atom-field coupling $\frac{U_0}{2}$ and pump strength η . It is the two center-of-mass motion modes that correspond to the two atomic internal levels involved in the Dicke model.

In this formalism, it is clear that the role of H_t is to induce transitions between different eigenstates of S_z (that is, the $|m\rangle$ ’s, $S_z|m\rangle = (m - \frac{N}{2})|m\rangle$), with amplitudes proportional to t . However, since $t \ll \frac{U_0}{2}, \kappa$, this process can be neglected in the short-time interval.

APPENDIX B: SOME USEFUL INEQUALITIES

We first introduce an inequality [21],

$$|\langle A^\dagger B \rangle|^2 \leq \langle A^\dagger A \rangle \langle B^\dagger B \rangle, \quad (\text{B1})$$

where A, B are two arbitrary operators (hermitian or non-hermitian), and the average is taken over an arbitrary state (pure or mixed). Let $A = a, B = I$ (unity operator) in Eq.(B1), we obtain

$$\langle a^\dagger \rangle \langle a \rangle \leq \langle a^\dagger a \rangle. \quad (\text{B2})$$

For steady states, we have this inequality plus the constraint Eq.(49), hence

$$\begin{aligned} \langle a^\dagger a \rangle_{st} &\geq \frac{1}{4} [(\langle a^\dagger \rangle_{st} + \langle a \rangle_{st})^2 - (\langle a^\dagger \rangle_{st} - \langle a \rangle_{st})^2] \\ &= \frac{1}{4} (\langle a^\dagger \rangle_{st} + \langle a \rangle_{st})^2 + \frac{\kappa^2}{\eta^2} \langle a^\dagger a \rangle_{st}^2 \\ &\geq \frac{\kappa^2}{\eta^2} \langle a^\dagger a \rangle_{st}^2, \end{aligned} \quad (\text{B3})$$

which yields an upper bound for the photon number

$$\langle a^\dagger a \rangle_{st} \leq \frac{\eta^2}{\kappa^2}. \quad (\text{B4})$$

This can be understood as the maximum photon number occurs when the probe is at resonance with the cavity.

We then show that it is legitimate to neglect the first term on the right hand side of Eq.(50), which is

$$\begin{aligned} &it \langle [a|m\rangle \langle m|, b_1^\dagger b_2 + b_2^\dagger b_1] \rangle_{st} \\ &= it f(m+1) \langle a|m\rangle \langle m+1| \rangle_{st} - it f(m+1) \langle a|m+1\rangle \langle m| \rangle_{st} \\ &\quad + it f(m) \langle a|m\rangle \langle m-1| \rangle_{st} - it f(m) \langle a|m-1\rangle \langle m| \rangle_{st}. \end{aligned} \quad (\text{B5})$$

It is ready to show that the ratios of the four terms to $-i\eta \langle |m\rangle \langle m| \rangle_{st}$ are at least of order t/κ , as long as $\langle |m\rangle \langle m| \rangle_{st}$ is of order unity. Let us take the third term for an example. Applying inequalities (B1) and (B4),

$$\begin{aligned} |it f(m) \langle a|m\rangle \langle m-1| \rangle_{st}| &\leq t f(m) [\langle a^\dagger a \rangle_{st} \langle |m\rangle \langle m| \rangle_{st}]^{1/2} \\ &\leq t f(m) \langle a^\dagger a \rangle_{st}^{1/2} \\ &\leq f(m) \left(\frac{t}{\kappa}\right) \eta, \end{aligned} \quad (\text{B6})$$

and similar results hold for the other three terms. This guarantees that the first term on the right hand of Eq.(50) is much less than the second term.

-
- [1] F. Brennecke, T. Donner, S. Ritter, T. Bourdel, M. Köhl, and T. Esslinger, *Nature* (London) (in press).
 - [2] Y. Colombe, T. Steinmetz, G. Dubois, F. Linke, D. Hunger, and J. Reichel, Preprint at <http://cn.arxiv.org/abs/0706.1390>.
 - [3] K. M. Fortier, S. Y. Kim, M. J. Gibbons, P. Ahmadi, and M. S. Chapman, *Phys. Rev. Lett.* **98**, 233601 (2007).
 - [4] S. Nußmann, M. Hijlkema, B. Weber, F. Rohde, G. Rempe, and A. Kuhn, *Phys. Rev. Lett.* **95**, 173602 (2005).
 - [5] I. B. Mekhov, C. Maschler, and H. Ritsch, *Nature Physics*. **3**, 319 (2007).
 - [6] J. Ye, D. W. Vernooy, and H. J. kimble, *Phys. Rev. Lett.* **83**, 4987 (1999).
 - [7] A. Öttl, S. Ritter, M. Köhl, and T. Esslinger, *Phys. Rev. Lett.* **95**, 090404 (2005); T. Bourdel, T. Donner, S. Ritter, A. Öttl, M. Köhl, and T. Esslinger, *Phys. Rev. A* **73**, 043602 (2006); S. Ritter, A. Öttl, T. Donner, T. Bourdel, M. Köhl, and T. Esslinger, *Phys. Rev. Lett.* **98**, 090402 (2007).
 - [8] C. Maschler and H. Ritsch, *Opt. Commun.* **243**, 145 (2004).
 - [9] S. M. Chumakov, A. B. Klimov, and C. Saavedra, *Phys. Rev. A* **61**, 033814 (2000).
 - [10] C. Maschler and H. Ritsch, *Phys. Rev. Lett.* **95**, 260401 (2005).
 - [11] W. Chen, D. Meiser, and P. Meystre, *Phys. Rev. A* **75**, 023812 (2007).
 - [12] G. J. Milburn, J. Corney, E. M. Wright, and D. F. Walls, *Phys. Rev. A* **55**, 4318 (1997).
 - [13] D. Jacksch, C. Bruder, J. I. Cirac, C. W. Gardiner, and P. Zoller, *Phys. Rev. Lett.* **81**, 3108 (1998).
 - [14] S. Gupta, K. L. Moore, K. W. Murch, and D. M. Stamper-Kurn, Preprint at <http://arxiv.org/abs/0706.1052> (2007).
 - [15] S. Kuhr, W. Alt, D. Schrader, M. Müller, V. Gomer, and D. Meschede, *Science* **293**, 278 (2001).
 - [16] I. Dotsenko, W. Alt, M. Khudaverdyan, S. Kuhr, D. Meschede, Y. Miroshnychenko, D. Schrader, and A. Rauschenbeutel, *Phys. Rev. Lett.* **95**, 033002 (2005).
 - [17] J. G. Peixoto de Faria and M. C. Nemes, *Phys. Rev. A* **69**, 063812 (2004).
 - [18] S. M. Tan, *J. Opt. B: Quantum Semiclass Opt.* **1**, 424 (1999).
 - [19] J. Beugnon, C. Tuchendler, H. Marion, A. Gaëtan, Y. Miroshnychenko, Y. R. P. Sortais, A. M. Lance, M. P. A. Jones, G. Messin, A. Browaeys, and P. Grangier, *Nature Physics* (published online).
 - [20] J. J. Sakurai, *Modern Quantum Mechanics*, revised version (Addison-Wesley, New York, 1994).
 - [21] R. R. Puri, *Mathematical Methods of Quantum Optics* (Springer, Berlin, 2001).